Available online at www.sciencedirect.com
ScienceDirect
Bioorganic & Medicinal Chemistry 16 (2008) 27–33
Bioorganic & Medicinal Chemistry

Spectroscopic properties of pyrene-containing DNA mimics

Florent Samain, Vladimir L. Malinovskii, Simon M. Langenegger and Robert Häner*

Department of Chemistry and Biochemistry, University of Bern, Freiestrasse 3, CH-3012 Bern, Switzerland

Received 8 August 2006; revised 16 October 2006; accepted 27 April 2007
Available online 3 May 2007

Abstract—DNA mimics containing non-nucleosidic pyrene building blocks are described. The modified oligomers form stable hybrids, although a slight reduction in hybrid stability is observed in comparison to the unmodified DNA duplex. The nature of the interaction between the pyrene residues in single and double stranded oligomers is analyzed spectroscopically. Intra- and interstrand stacking interactions of pyrenes are monitored by UV-absorbance as well as fluorescence spectroscopy. Excimer formation is observed in both single and double strands. In general, intrastrand excimers show fluorescence emission at shorter wavelengths (approx. 5–10 nm) than excimers formed by interstrand interactions. The existence of two different forms of excimers (intra- vs. interstrand) is also revealed in temperature dependent UV-absorbance spectra.

1. Introduction

Modified oligonucleotides enjoy widespread interest as diagnostic and research tools.[1,2] In addition, the generation of defined molecular architectures using nucleic acid-like building blocks is a research topic of high interest.[3–8] The repetitive and well-defined structural features of nucleic acids and related types of oligomers renders them valuable building blocks for the generation of nanometer-sized structures.[9] The combination of the natural nucleotides with novel, synthetic building blocks lead to a large increase in the number of possible constructs and applications.[10,11] Recently, we reported the synthesis and properties of non-nucleosidic, phenanthrene-based building blocks and their incorporation into DNA.[12,13] These building blocks can serve as base surrogates allowing hybridisation of complementary strands without significant destabilization of the duplex. Replacement of two or more base pairs by non-nucleosidic phenanthrene building blocks is well tolerated having almost no influence on hybrid stability compared to an unmodified duplex.[14] Based on spectroscopic data, a model of interstrand stacked polyaromatic building blocks was derived. Interstrand stacking of such non-nucleosidic polyaromatic building blocks was subsequently shown by excimer formation[15] of pyrenes placed in opposite positions.[16] Interstrand stacking arrangement of a similar type of non-nucleosidic pyrene building blocks was shown by NMR investigations.[17] Furthermore, natural DNA is also known to adopt an interstrand stacking structure, the *i-motif*, which is formed by association of stretches of two or more cytidines involving base intercalation.[18] Due to their spectroscopic properties, the use of pyrene building blocks is interesting with regard to the fluorescence features of the resulting oligomers and the hybrids they form.[19–35] Some notable examples of extra-helical arrangement of pyrenes along the backbones of DNA[19,35] and RNA[20] were described recently. The absorption spectrum of pyrene overlaps only partially with oligonucleotide absorption and the fluorescence is strongly dependent on local changes. Within the set of building blocks that we have been using (phenanthrene, phenanthroline[36,37] and pyrene) the pyrene molecule is, thus, an ideal candidate for probing the stacking interactions of polyaromatic building blocks in DNA. Here, we report the synthesis and spectroscopic investigation of DNA mimics containing multiple pyrene building blocks.

2. Results and discussion

Along with geometrical constraints of the sugar phosphate backbone, stacking interactions and hydrogen bonding are the most important factors responsible for the self organization of single stranded nucleic acids into

Keywords: Pyrene; DNA; Mimic; Fluorescence; Excimer.
* Corresponding author. Fax: +41 31 631 8057; e-mail: robert.haener@ioc.unibe.ch

0968-0896/$ - see front matter © 2007 Elsevier Ltd. All rights reserved.
doi:10.1016/j.bmc.2007.04.052

double helical structures.[38–40] The type of modified DNA described here is based on the use of extended aromatic systems with non-nucleosidic linkers. In this system, the stacking properties can be considered as the main factor for stabilization of secondary structures. Due to their hydrophobic nature, stacking interactions of the *pyrene–pyrene* and/or *base–pyrene* type are expected to play an important role not only in duplex but also in single strands in polar medium. Aggregation of pyrenes in aqueous solutions has been a topic of intensive investigation in the past and was reviewed by *Winnik*.[15] These findings serve as an excellent basis for interpretation of pyrenes embedded in an oligonucleotide based system. In the following, we will divide the description of our results into two parts, that is, the spectroscopic investigation of pyrene-containing (i) single strands and (ii) double stands. This will allow differentiating characteristics which are due either to *intramolecular* or to *intermolecular* stacking of the pyrenes.

2.1. Thermal denaturation experiments

Before investigating the spectroscopic properties of pyrene-containing oligomers, the stability of hybrids was tested by thermal denaturation. The data are summarized in Table 1. Oligonucleotides **1** and **2** serve as controls and oligomers **3**–**8** contain between one and three pyrene building blocks per single strand. T_m values show a picture that is in agreement with previous findings with phenanthrene-modified oligomers,[14,36] that is, a slight decrease in hybrid stability if one to three pairs of pyrenes are placed in opposite positions in the middle of the duplex. Values for ΔT_m per modification ranging between 0.6 and 1.9 °C were observed. The destabilization resulting from removal of natural base pairs is, thus, largely compensated by aryl–aryl stacking interactions between the pyrene residues. T_m values were also determined at two further wavelengths (245 and 354 nm, see Supplementary data). The T_ms obtained at these wavelengths correlate very well with the ones at 260 nm, indicating a cooperative melting process.

2.2. Pyrene-containing single strands

We next performed a set of temperature-dependent UV–vis and fluorescence experiments with single stranded oligonucleotides to investigate the intrastrand interactions of pyrenes. Representative data are shown in Figures 1 and 2, respectively. Interactions between pyrene and nucleobase(s) can be observed in the temperature-dependent experiments (Fig. 1). Increasing temperatures are associated with an increase in absorbance as well as with a blue-shift in maximum absorbance in the range 300–400 nm, which corresponds to pyrene absorbance. These findings are in agreement with a reduction in π-stacking with increasing temperature, since stacking interactions among chromophores are generally accompanied with (i) a decrease in the absorbance intensity (hypochromic effect), (ii) a broadening of signals and (iii) a red-shift.[15,41] While a broadening is not clearly detectable, the other two characteristics are obviously present: a red-shift of 10 nm is observed for **3** upon going from 90 to 10 °C and it is concomitant with a decrease in absorbance intensity. The gradual change in temperature leads to an isosbestic point at 360 nm. As expected, temperature dependent fluorescence data (Fig. 2a show the monomer fluorescence (around 400 nm), which is typical for pyrene monomer fluorescence. The absence of distinct bands at longer wavelength reveals that there is no dominant intrastrand exciplex formation in single strand **3**; due to the asymmetry of the bands towards longer wavelength, exciplex can, however, not be ruled out completely.[15] The intensity of absorbance spectra of the single strand **4** is essentially the same but fluorescence is of lower intensity (approx. 50% compared to **3**, see Supplementary data). This is well in agreement with findings that guanine (neighbouring base to pyrene in oligomer **4**, only), but not adenine or cytosine, acts as an efficient quencher of pyrene fluorescence.[42]

Table 1. Influence of non-nucleosidic pyrene building blocks on hybrid stability[a]

Entry	Oligo #	Duplex	T_m (°C)	ΔT_m	ΔT_m per modification
1	**1**	(5′) AGC TCG GTC ATC GAG AGT GCA	69.5	—	—
	2	(3′) TCG AGC CAG TAG CTC TCA CGT			
2	**3**	(5′) AGC TCG GTC A**S**C GAG AGT GCA	68.9	−0.6	−0.6
	4	(3′) TCG AGC CAG T**S**G CTC TCA CGT			
3	**5**	(5′) AGC TCG GTC **SS**C GAG AGT GCA	66.2	−3.3	−1.7
	6	(3′) TCG AGC CAG **SS**G CTC TCA CGT			
4	**7**	(5′) AGC TCG GT**S SS**C GAG AGT GCA	63.8	−5.7	−1.9
	8	(3′) TCG AGC CA**S SS**G CTC TCA CGT			

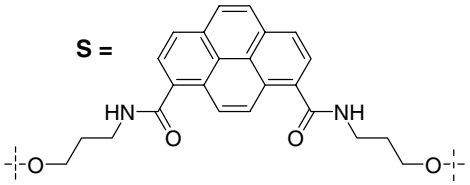

[a] Conditions: 1.0 μM oligonucleotide concentration (each strand), 10 mM Tris–HCl buffer (pH 7.4) and 100 mM NaCl; 0.5 °C/min; absorbance measured at 260 nm.

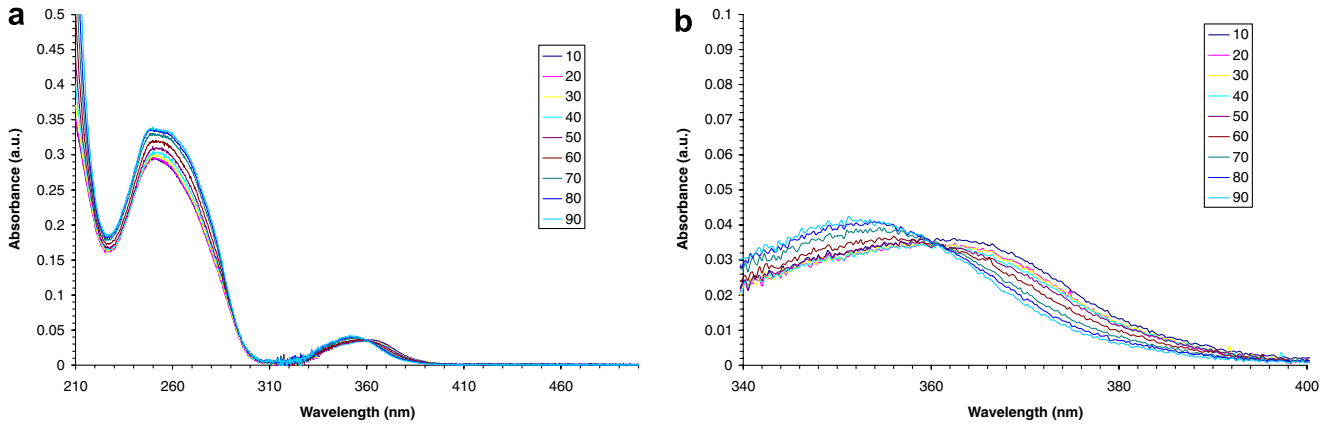

Figure 1. Temperature-dependent UV-absorbance of oligomer **3** (left, full spectrum) showing an isosbestic point at 360 nm (right); for conditions see Table 1.

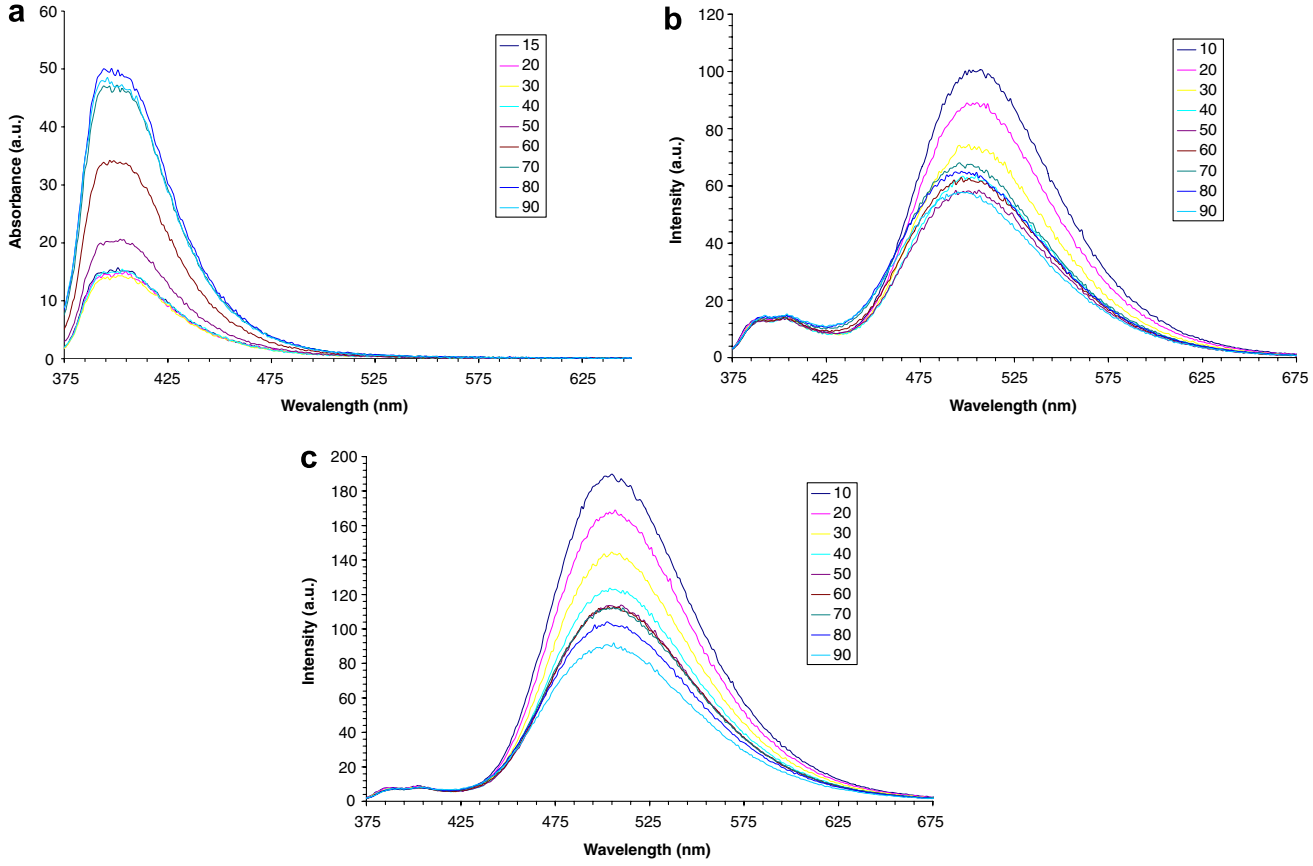

Figure 2. Temperature-dependent fluorescence spectra of single strands **3** (a), **5** (b) and **7** (c); for conditions, see Table 1.

Upon addition of further pyrenes, observation of pyrene–pyrene interactions in single strands is rendered possible. Fluorescence data of **5** are shown in Figure 2b. As expected, a strong excimer band with a maximum emission at 505 nm appears while monomer fluorescence (around 400 nm) is greatly reduced. This indicates strong stacking interactions between the adjacent pyrenes in the single strand. For oligomer **7**, which contains three consecutive pyrenes, this trend continues. The fluorescence spectrum (Fig. 2c) shows essentially only excimer emission at 506 nm. A noteworthy difference between the two oligomers **5** and **7** exists: while a temperature dependent change of the emission maximum in **5** (from 505 nm at 10 °C to 498 nm at 90 °C) is observed, the maximum remains more or less unchanged over the same temperature range for oligomer **7**. This finding is best explained in terms of "static" (or dimeric in ground state) and "dynamic" (monomeric in ground state) excimers[15], since the latter type shows a blue-shifted emission in comparison to the static excimer. In oligomer **5**, which contains two pyrenes, increasing temperature leads to a larger separation of the pyrenes, hence they form a dynamic excimer on irradiation. In oligomer **7** separation of all pyrenes is less likely

and, over the investigated temperature range, the static excimer is dominating.[15] As observed with **3**, both oligomers **5** and **7** show an isosbestic point (362 and 361 nm, respectively) in the temperature-dependent absorbance spectrum (see Supplementary data).

2.3. Investigation of pyrene containing hybrids

As described above, the pyrene unit(s) participate strongly in intrastrand stacking interactions. The question arises whether the same (intrastrand) interactions persist upon hybridisation or if different (interstrand) pyrene interactions become dominant. While this question was partly answered previously for hybrid **3*****4** by observation of excimer formation by interstrand stacking of two pyrenes,[16a] the behaviour of single strands containing multiple pyrenes might be different. To study this question, temperature dependent absorbance and fluorescence experiments with the different hybrids were performed. Temperature dependent fluorescence properties of pyrene of nucleic acids containing multiple, extrahelical pyrene residues have been used to study pyrene aggregation.[19,20] The absorbance spectrum of hybrid **3*****4** (Fig. 3) shows that the two pyrene units of the single strands are involved in stacking interactions. First, the expected blue-shift is observed with increasing temperature (see Figure 3b, showing the range of 340–400 nm).[43] The maximum absorbance decreases from 357 nm at 10 °C to 352 nm at 90 °C. More importantly, two isosbestic points are present, indicating two different types of interaction between the pyrenes. The first isosbestic point (366 nm) formed by curves taken below the melting temperature (68.9 °C, Table 1) can be attributed to decreasing association between the pyrenes with increasing temperature. The second isosbestic point is formed at a shorter wavelength (362 nm) and is formed by the curves taken above the T_m and, therefore, has its origin in changes occurring within the single strands. The observed value of the blue-shifted isosbestic point correlates well with the one observed with single strand **3** alone (360 nm, see above).

The temperature dependent fluorescence spectra of hybrid **3*****4** (Fig. 4) confirm this interpretation. A strong excimer band at 500 nm, arising from interstrand stacking interactions between the two pyrenes, gradually replaced by pyrene monomer emission at higher temperature. At temperatures above the T_m (68.9 °C), only monomer fluorescence is observed.

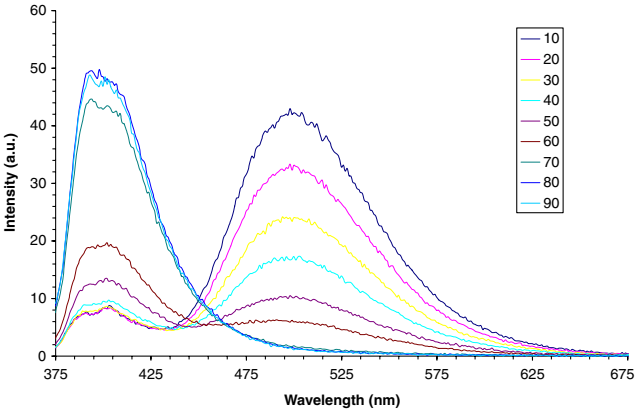

Figure 4. Temperature dependent fluorescence spectra of hybrid **3*****4**; for conditions see Table 1.

As expected, the hybrids with four (**5*****6**) and six (**7*****8**) pyrenes show a rather different temperature dependence in their fluorescence spectra (Fig. 5) giving rise only to excimer emission, also at temperatures above the T_m. Below the T_m, the emission intensity is decreasing with increasing temperature, indicating a weakening of (or a geometrical change in) the association of the pyrenes. In addition, the maximum emission in the hybrids (i.e., below the T_m) is at higher wavelength than the one in the single strands (i.e., above the T_m). The changes in the maximum emission over the temperature range investigated are from 514 to 500 nm in hybrid **5*****6** and 512–505 nm in hybrid **7*****8**. The temperature dependent absorbance spectra of hybrids **5*****6** and **7*****8** (see Supplementary data) are very similar to the one of hybrid **3*****4**. Thus, both hybrids also show two isosbestic points representing the single and the double stranded states. Finally, all hybrids showed circular dichroism spectra typical for B-DNA (data not shown).

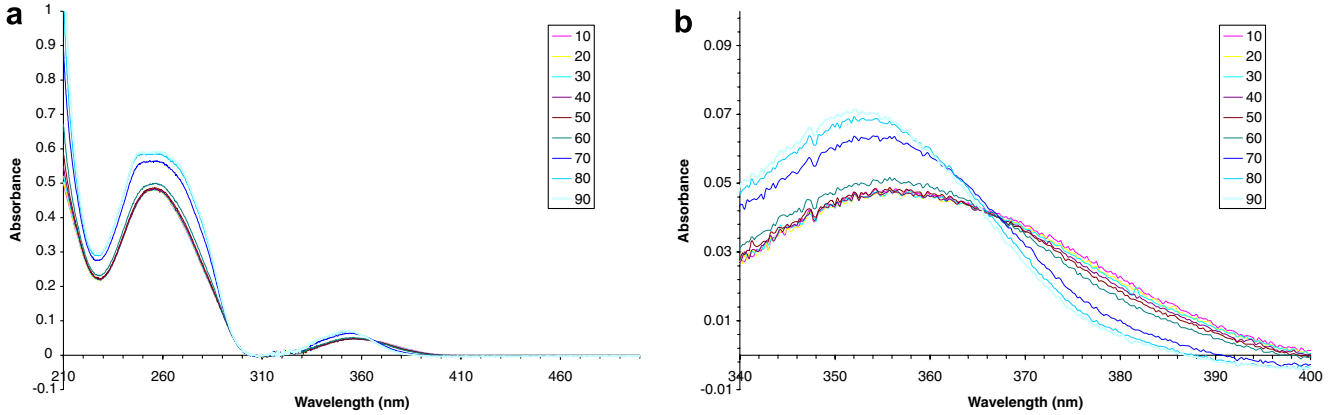

Figure 3. Temperature dependent absorbance spectra of hybrid **3*****4** (left: full spectrum, right: enlargement of the range 340–400 nm; for conditions see Table 1.

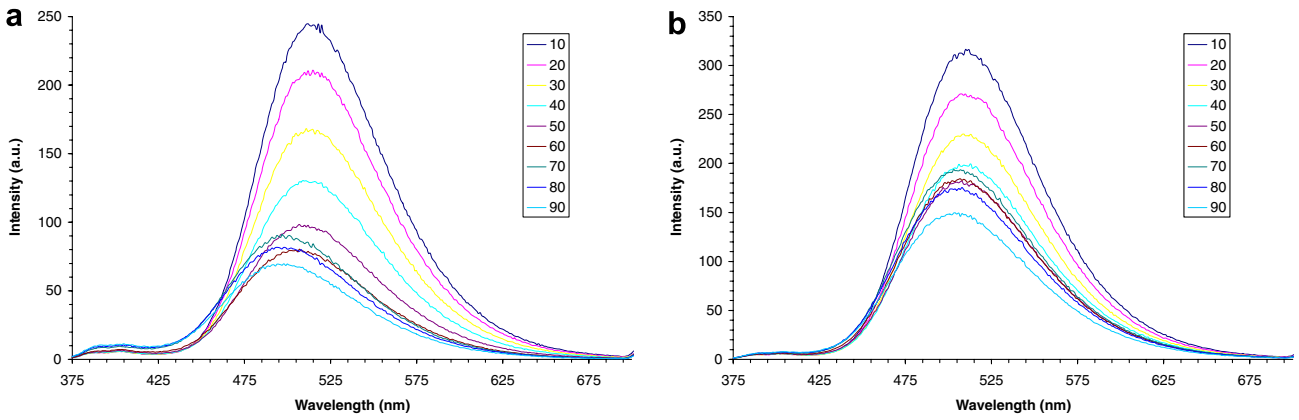

Figure 5. Emission spectra of hybrids **5**∗**6** (left) and **7**∗**8** (right); for conditions see Table 1.

3. Conclusions

DNA mimics containing non-nucleosidic, polyaromatic pyrene building blocks have been investigated spectroscopically. Absorbance and emission spectra provide insight into the interactions among pyrenes or between pyrene and neighbouring nucleic acid bases. Investigation of single strands showed that *intrastrand* excimer formation takes place if two or three pyrenes are placed in adjacent positions. In hybrids, interstrand excimers are formed. In general, intrastrand excimers show fluorescence emission at shorter wavelengths (498–505 nm) than the excimers formed by interstrand interactions (505–514 nm). The existence of two different forms of excimers (intra- vs. interstrand) is also revealed by temperature dependent UV-absorbance spectra. A gradual shift of maximum absorbance is accompanied by appearance of two isosbestic points, one of which (at longer wavelength) can be attributed to interstrand stacking in the hybrid and the second from intrastrand stacking in the single strands. Thus, as in natural single stranded nucleic acids, DNA mimics containing the type of modified building block described herein are organized by stacking interactions. Upon duplex formation, however, the DNA mimics behave differently, because the intrastrand interactions cede to the more favourable interstrand stacking. The hybridisation process of the DNA mimics is, thus, not aided—at least not to the same extent as in natural DNA—by the preorganization of the single strands. The denaturation process of the pyrene containing DNA mimics is illustrated in Scheme 1. In addition to giving insight into the intrastrand and interstrand interactions the described pyrene building blocks allow the design and construction of DNA mimics with interesting spectroscopic properties for applications as diagnostic tools and as novel materials.

4. Experimental

The required pyrene building block with a three-carbon linker was synthesized according to the published procedure.[16a] Nucleoside phosphoramidites from *Transgenomic* (Glasgow, UK) were used for oligonucleotide synthesis. Oligonucleotides **1**–**8** were prepared via automated oligonucleotide synthesis by a standard synthetic procedure ('trityl-off' mode) on a 394-DNA/RNA synthesizer (*Applied Biosystems*). Cleavage from the solid support and final deprotection was done by treatment with 30% NH_4OH solution at 55 °C overnight. All oligonucleotides were purified by reverse phase HPLC (LiChrospher 100 *RP-18*, 5 μm, Merck), *Bio-Tek Instruments Autosampler 560*); eluent $A = (Et_3NH)OAc$ (0.1 M, pH 7.4); eluent B = MeCN; elution at 40 °C; gradient 5–20% B over 30 min.

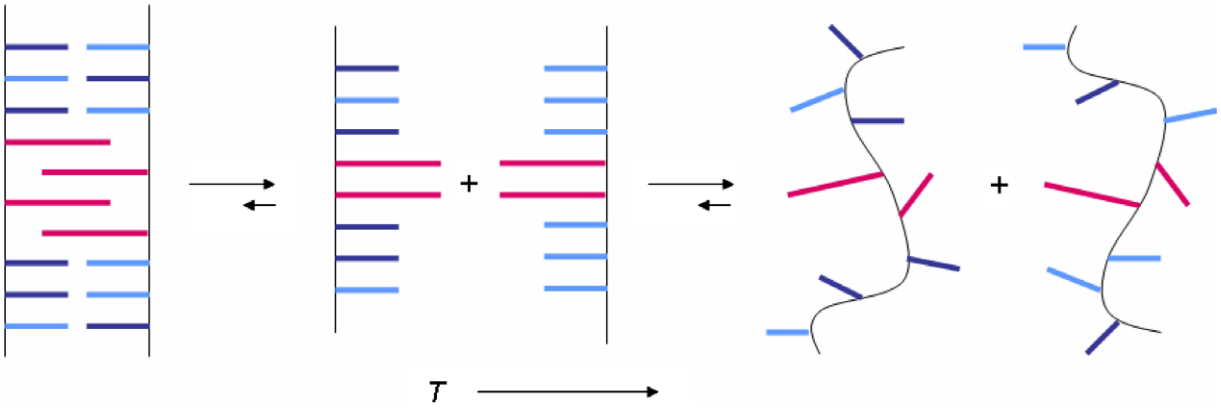

Scheme 1. Illustration of the denaturation process of pyrene containing DNA mimics from interstrand stacked pyrenes (red) in the duplex to intrastrand stacked pyrenes in the single strands and random coils at high temperature (natural bases illustrated in blue).

Molecular mass determinations of oligonucleotides were performed with a Sciex QSTAR pulsar (hybrid quadrupole time-of-flight mass spectrometer, *Applied Biosystems*). ESI–MS (negative mode, CH_3CN/H_2O/TEA) data of compounds **1**–**8** are presented in Supplementary data.

Thermal denaturation experiments (1.0 μM oligonucleotide concentration (each strand), 10 mM Tris–HCl buffer (pH 7.4) and 100 mM NaCl) were carried out on *Varian Cary-100 Bio*-UV/vis spectrophotometer equipped with a *Varian Cary*-block temperature controller and data were collected with Varian WinUV software at 245, 260 and 354 nm (cooling–heating–cooling cycles in the temperature range of 20–90 °C, temperature gradient of 0.5 °C/min). Data were analyzed with *Kaleidagraph*® software from ©*Synergy Software*. Melting temperature (T_m) values were determined as the maximum of the first derivative of the smoothed (window size 3) melting curve.

Temperature dependent UV–vis spectra were collected over the range of 210–500 nm at 10–90 °C with a 10 °C interval on*Varian Cary-100 Bio*-UV/vis spectrophotometer equipped with a *Varian Cary*-block temperature controller. All experiments were carried out at a 1.0 μM oligonucleotide concentration (each strand) in Tris–HCl buffer (10 mM) and NaCl (100 mM) at pH 7.4. The cell compartment was flushed with N_2 to avoid water condensation at low temperature.

Temperature dependent fluorescence data were collected for 1.0 μM oligonucleotide (1.0 μM of each strand in case of double strands) solutions in Tris–HCl buffer (10 mM) and NaCl (100 mM) at pH 7.4 on a Varian Cary Eclipse fluorescence spectrophotometer equipped with a Varian Cary-block temperature controller (excitation at 354 nm; excitation and emission slit width of 5 nm). Varian Eclipse software was used to investigate the fluorescence of the different pyrene-containing oligonucleotides at a wavelength range of 375–700 nm in the temperature range of 10–90 °C.

Acknowledgment

Financial support by the Swiss National Science Foundation (Grant 200020-109482) is gratefully acknowledged.

Supplementary data

Supplementary data associated with this article can be found, in the online version, at doi:10.1016/j.bmc.2007.04.052.

References and notes

1. Verma, S.; Jager, S.; Thum, O.; Famulok, M. *Chem. Rec.* **2003**, *3*, 51–60.
2. Kohler, O.; Jarikote, D. V.; Singh, I.; Parmar, V. S.; Weinhold, E.; Seitz, O. *Pure Appl. Chem.* **2005**, *77*, 327–338.
3. Seeman, N. C. *Nature* **2003**, *421*, 427–431.
4. Samori, B.; Zuccheri, G. *Angew. Chem. Int. Ed.* **2005**, *44*, 1166–1181.
5. Shih, W. M.; Quispe, J. D.; Joyce, G. F. *Nature* **2004**, *427*, 618–621.
6. Mirkin, C. A. *Inorg. Chem.* **2000**, *39*, 2258–2272.
7. Chworos, A.; Severcan, I.; Koyfman, A. Y.; Weinkam, P.; Oroudjev, E.; Hansma, H. G.; Jaeger, L. *Science* **2004**, *306*, 2068–2072.
8. Claridge, S. A.; Goh, S. L.; Frechet, J. M. J.; Williams, S. C.; Micheel, C. M.; Alivisatos, A. P. *Chem. Mater.* **2005**, *17*, 1628–1635.
9. Wengel, J. *Org. Biomol. Chem.* **2004**, *2*, 277–280.
10. Eschenmoser, A. *Chimia* **2005**, *59*, 836–850.
11. Herdewijn, P. *Biochim. Biophys. Acta, Gene Struct. Expr.* **1999**, *1489*, 167–179.
12. Langenegger, S. M.; Häner, R. *Helv. Chim. Acta* **2002**, *85*, 3414–3421.
13. Langenegger, S. M.; Bianke, G.; Tona, R.; Häner, R. *Chimia* **2005**, *59*, 794–797.
14. Langenegger, S. M.; Häner, R. *ChemBioChem* **2005**, *6*, 2149–2152.
15. Winnik, F. M. *Chem. Rev.* **1993**, *93*, 587–614.
16. (a) Langenegger, S. M.; Häner, R. *Chem. Commun.* **2004**, 2792–2793; (b) Langenegger, S. M.; Häner, R. *Bioorg. Med. Chem. Lett.* **2006**, *16*, [Epub ahead of print].
17. Nielsen, C. B.; Petersen, M.; Pedersen, E. B.; Hansen, P. E.; Christensen, U. B. *Bioconjug. Chem.* **2004**, *15*, 260–269.
18. Gueron, M.; Leroy, J. L. *Curr. Opin. Struct. Biol.* **2000**, *10*, 326–331.
19. Mayer-Enthart, E.; Wagenknecht, H. A. *Angew. Chem. Int. Ed.* **2006**, *45*, 3372–3375.
20. Nakamura, M.; Ohtoshi, Y.; Yamana, K. *Chem. Commun.* **2005**, 5163–5165.
21. Malakhov, A. D.; Skorobogatyi, M. V.; Prokhorenko, I. A.; Gontarev, S. V.; Kozhich, D. T.; Stetsenko, D. A.; Stepanova, I. A.; Shenkarev, Z. O.; Berlin, Y. A.; Korshun, V. A. *Eur. J. Org. Chem.* **2004**, 1298–1307.
22. Filichev, V. V.; Vester, B.; Hansen, L. H.; Pedersen, E. B. *Nucleic Acids Res.* **2005**, *33*, 7129–7137.
23. Balakin, K. V.; Korshun, V. A.; Mikhalev, I. I.; Maleev, G. V.; Malakhov, A. D.; Prokhorenko, I. A.; Berlin, Y. A. *Biosens. Bioelectron.* **1998**, *13*, 771–778.
24. Yamana, K.; Iwai, T.; Ohtani, Y.; Sato, S.; Nakamura, M.; Nakano, H. *Bioconjug. Chem.* **2002**, *13*, 1266–1273.
25. Michel, J.; Bathany, K.; Schmitter, J. M.; Monti, J. P.; Moreau, S. *Tetrahedron* **2002**, *58*, 7975–7982.
26. Dioubankova, M. N.; Malakhov, A. D.; Stetsenko, D. A.; Gait, M. J.; Volynsky, P. E.; Efremov, R. G.; Korshun, V. A. *ChemBioChem* **2003**, *4*, 841–847.
27. Hrdlicka, P. J.; Babu, B. R.; Sorensen, M. D.; Wengel, J. *Chem. Commun.* **2004**, 1478–1479.
28. Fujimoto, K.; Shimizu, H.; Inouye, M. *J. Org. Chem.* **2004**, *69*, 3271–3275.
29. Okamoto, A.; Ichiba, T.; Saito, I. *J. Am. Chem. Soc.* **2004**, *126*, 8364–8365.
30. Kosuge, M.; Kubota, M.; Ono, A. *Tetrahedron Lett.* **2004**, *45*, 3945–3947.
31. Yamana, K.; Fukunaga, Y.; Ohtani, Y.; Sato, S.; Nakamura, M.; Kim, W. J.; Akaike, T.; Maruyama, A. *Chem. Commun.* **2005**, 2509–2511.
32. Okamoto, A.; Ochi, Y.; Saito, I. *Chem. Commun.* **2005**, 1128–1130.
33. Cho, Y. J.; Kool, E. T. *ChemBioChem* **2006**, *7*, 669–672.
34. Kashida, H.; Asanuma, H.; Komiyama, M. *Chem. Commun.* **2006**, 2768–2770.

35. Barbaric, J.; Wagenknecht, H. A. *Org. Biomol. Chem.* **2006**, *4*, 2088–2090.
36. Langenegger, S. M.; Häner, R. *Tetrahedron Lett.* **2004**, *45*, 9273–9276.
37. Langenegger, S. M.; Häner, R. *ChemBioChem* **2005**, *6*, 848–851.
38. Saenger, W. *Principles of Nucleic Acid Structure*; Springer-Verlag: New York, 1984.
39. Kool, E. T. *Chem. Rev.* **1997**, *97*, 1473–1487.
40. Farwer, J.; Packer, M. J.; Hunter, C. A. *Biopolymers* **2006**, *81*, 51–61.
41. For a recent example of a redshift in absorbance upon DNA duplex formation and pyrene intercalation by oligonucleotides containing a single pyrene modification, see Nakamura, M.; Fukunaga, Y.; Sasa, K.; Ohtoshi, Y.; Kanaori, K.; Hayashi, H.; Nakano, H.; Yamana, K. *Nucleic Acids Res.* **2005**, *33*, 5887–5895.
42. See, for example Donho, C.; Saito, I. In *Charge Transfer in DNA—From Mechanism to Application*; Wagenknecht, H. A., Ed.; Chapter 7—Chemical Approach to Modulating Hole Transport Through DNA; Wiley-VCH: Weinheim, Germany, 2005; pp 153–174.
43. It should be noted that, principally, the same observations are possible at the other major pyrene absorbance band around 245 nm; since interpretations of this region are complicated by the overlap with the spectrum of the natural bases, however, only the region of 300–400 nm is described here.